Report

Current Biology

Shoot-to-Root Mobile Transcription Factor HY5 Coordinates Plant Carbon and Nitrogen Acquisition

Graphical Abstract

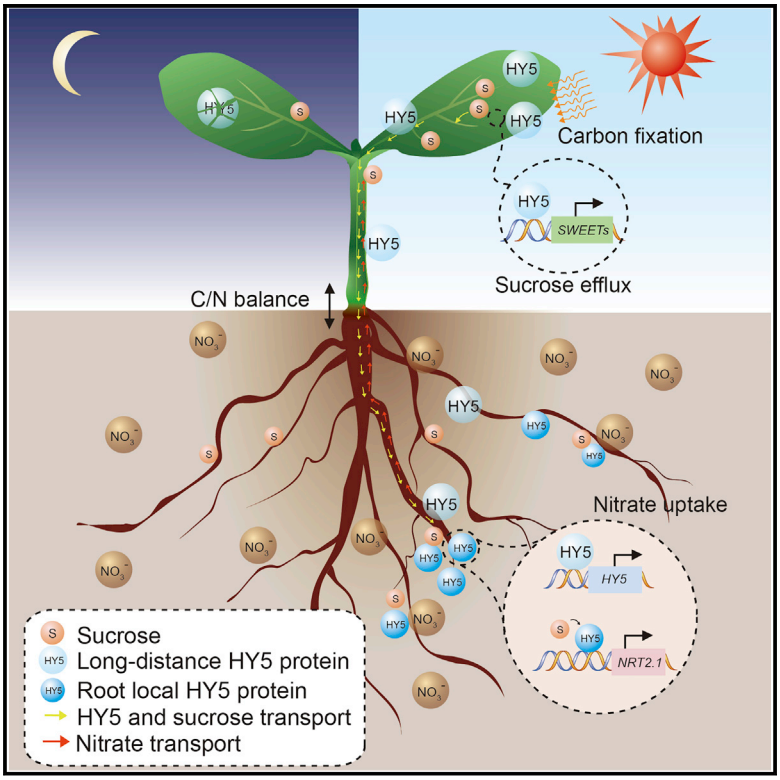

Highlights

- HY5 is essential for light-responsive coordination of the growth of shoots and roots
- Shoot-to-root translocated HY5 mediate light-activated root growth and N uptake
- Carbohydrate photosynthate-induced *NRT2.1* expression and N uptake depend upon HY5
- HY5 contributes to maintain balance of C and N metabolism at varying light fluence

Authors

Xiangbin Chen, Qinfang Yao, Xiuhua Gao, Caifu Jiang, Nicholas P. Harberd, Xiangdong Fu

Correspondence

xdfu@genetics.ac.cn

In Brief

Chen et al. show that transcription factor HY5 is a shoot-to-root mobile signal that mediates light-responsive coupling of shoot growth and C assimilation with root growth and N uptake in *Arabidopsis*. HY5 mobility thus contributes to maintain homeostatic balance between whole-plant C and N metabolism in response to a fluctuating environment.

Chen et al., 2016, Current Biology *26*, 640–646
March 7, 2016
http://dx.doi.org/10.1016/j.cub.2015.12.066

CellPress

CellPress

Current Biology
Report

Shoot-to-Root Mobile Transcription Factor HY5 Coordinates Plant Carbon and Nitrogen Acquisition

Xiangbin Chen,[1] Qinfang Yao,[1] Xiuhua Gao,[1] Caifu Jiang,[1,3] Nicholas P. Harberd,[2] and Xiangdong Fu[1,*]
[1]The State Key Laboratory of Plant Cell and Chromosome Engineering, Institute of Genetics and Developmental Biology, Chinese Academy of Sciences, Beijing 100101, China
[2]Department of Plant Sciences, University of Oxford, South Parks Road, Oxford OX1 3RB, UK
[3]Present address: Center for Life Sciences, China Agricultural University, Beijing 100193, China
*Correspondence: xdfu@genetics.ac.cn
http://dx.doi.org/10.1016/j.cub.2015.12.066

SUMMARY

Coordination of shoot photosynthetic carbon fixation with root inorganic nitrogen uptake optimizes plant performance in a fluctuating environment [1]. However, the molecular basis of this long-distance shoot-root coordination is little understood. Here we show that *Arabidopsis* ELONGATED HYPOCOTYL5 (HY5), a bZIP transcription factor that regulates growth in response to light [2, 3], is a shoot-to-root mobile signal that mediates light promotion of root growth and nitrate uptake. Shoot-derived HY5 auto-activates root *HY5* and also promotes root nitrate uptake by activating *NRT2.1*, a gene encoding a high-affinity nitrate transporter [4]. In the shoot, HY5 promotes carbon assimilation and translocation, whereas in the root, HY5 activation of *NRT2.1* expression and nitrate uptake is potentiated by increased carbon photoassimilate (sucrose) levels. We further show that HY5 function is fluence-rate modulated and enables homeostatic maintenance of carbon-nitrogen balance in different light environments. Thus, mobile HY5 coordinates light-responsive carbon and nitrogen metabolism, and hence shoot and root growth, in a whole-organismal response to ambient light fluctuations.

RESULTS AND DISCUSSION

Although plant shoots and roots follow distinct developmental trajectories, their biology is tightly coordinated to optimize whole-plant performance in a fluctuating environment. The coordination of metabolic assimilation is of key importance: shoots fix atmospheric carbon (C; CO_2), roots acquire soil ionic nitrogen (N; predominantly nitrate, NO_3^-) [1]. Because N is essential, soil NO_3^- levels frequently limit productivity in natural and agricultural environments [5, 6]. The regulation of rates of N and C acquisition is known to be tightly coupled [7, 8], with light regulating both processes [9]. However, the molecular mechanisms of the underlying regulatory long-distance shoot-root communication remain unknown.

HY5 Is Essential for Shoot-Illumination Promotion of Root Growth and NO_3^- Uptake

As a visible reporter of regulatory shoot-root communication, and because roots are not usually exposed to light, we determined the effects of separate illumination of shoots or roots on root growth of 3-day-old seedlings, which were then exposed to 3 days of differential light treatment (Figures 1A and S1A). We found that the primary roots of wild-type (WT) *Arabidopsis thaliana* (Col-0 laboratory strain) seedlings whose shoots (only) were exposed to light [S(L)/R(D)] were of a similar length to those of WT seedlings fully exposed to light [S(L)/R(L); Figures 1B and 1C]. In contrast, the roots of WT S(D)/R(L) seedlings were shorter than those of S(L)/R(D) seedlings and of a similar length to S(D)/R(D) seedlings (Figures 1B and 1C). In addition, lateral root proliferation of S(L)/R(D) seedlings was similar to that of S(L)/R(L), whereas lateral root proliferation of S(D)/R(L) seedlings was much less and similar to that of S(D)/R(D) (Figure S1B). Thus, shoot illumination promotes root growth, most likely via shoot-to-root signaling.

We next screened for *A. thaliana* mutants specifically disrupted in shoot illumination promoted root growth, and we found that one of them contained a new *HY5* loss-of-function allele (*hy5-526*; Figures 1B, S2A, and S2B). Further analysis showed that a *hy5* null allele also abolishes shoot-illumination-promoted root growth [10] (Figure 1C). *HY5* encodes the photomorphogenic bZIP transcription factor HY5 [2, 3]. HY5 is regulated by the COP1 ubiquitin ligase, which targets HY5 for proteolytic degradation in the dark [11]. Accordingly, we found that the loss-of-function *cop1-4* mutant mimics shoot-illumination promotion of root growth in dark-grown seedlings (Figure 1C). These results suggest that HY5 mediates shoot-illumination promotion of root growth.

We next found that WT root NO_3^- uptake is promoted by illumination of the shoot, but not of the root (Figure 1D). NO_3^- is taken up by plants via dual low-affinity/high-affinity CHL1/NRT1.1 and high-affinity NRT2.1 transporters [4, 12–15]. Shoot-illumination-promoted NO_3^- uptake was greatly diminished in the *nrt2.1-2* mutant lacking NRT2.1 [4] (Figure 1D) but relatively unaffected in a *chl1-5* mutant lacking CHL1/NRT1.1 [13] (Figure 1D), indicating that shoot-illumination promotion of root NO_3^- uptake is predominantly NRT2.1 dependent. Furthermore, shoot-illumination-promoted root NO_3^- uptake was largely abolished in both *hy5* and *hy5-526* (Figure 1D), suggesting that HY5 regulates NRT2.1-dependent shoot-illumination promotion of root NO_3^- uptake.

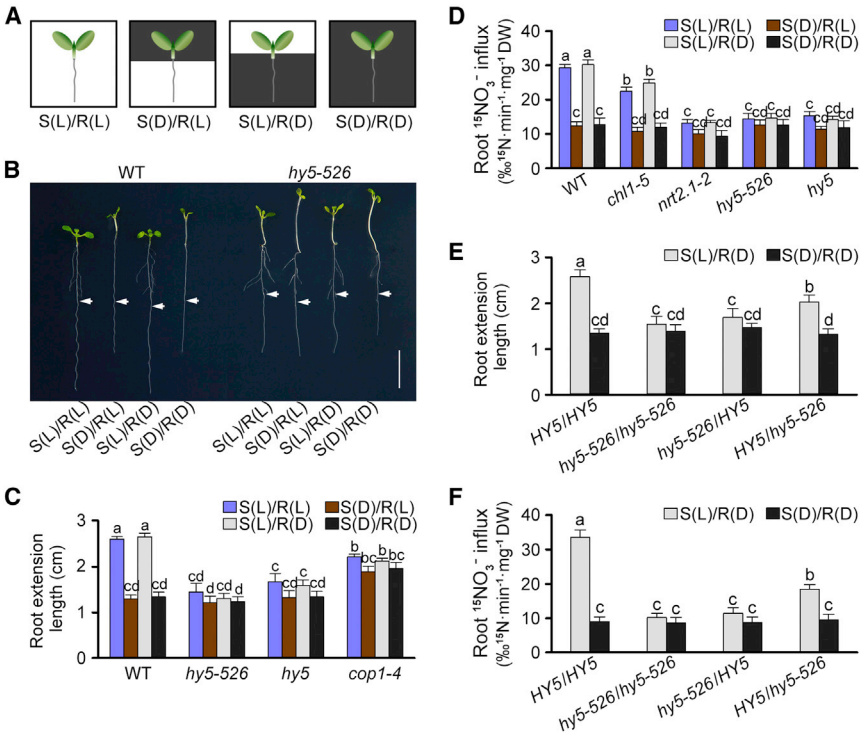

Figure 1. HY5 Mediates Shoot-Illumination Promotion of Root Growth and NRT2.1-Dependent NO_3^- Uptake

(A) Representation of differential shoot/root-illumination conditions. 3-day-old seedlings were exposed to 3 days of differential light treatment (100 μmol • s^{-1} • m^{-2}): shoot illuminated [S(L)] or dark grown [S(D)] and root illuminated [R(L)] or dark grown [R(D)] (see also Figure S1A).

(B) Differential shoot/root-illumination effects on WT and *hy5-526* primary root growth (see Figure S1B for lateral root growth). Arrowheads indicate the root-tip position at the beginning of the experiment. Scale bar, 1 cm.

(C) Differential shoot/root-illumination effects on WT, *hy5-526*, *hy5*, and *cop1-4* seedling primary root extension length.

(D) Differential shoot/root-illumination effects on $^{15}NO_3^-$ uptake of seedling roots.

(E) Differential shoot/root-illumination effects on primary root extension length of 10-day-old grafted plants. Grafts are indicated as scion/stock (e.g., *HY5/hy5-526* has a *HY5* scion and a *hy5-526* stock).

(F) Differential shoot/root-illumination effects on $^{15}NO_3^-$ uptake of roots of plants grafted as in (E).

(C–F) Data are shown as mean ± SEM (n = 30). The same lowercase letter denotes a non-significant difference between means ($p < 0.05$).

See also Figure S1.

HY5 Moves from Shoot to Root to Mediate Light-Activated Promotion of Root Growth and NO_3^- Uptake

Subsequent experiments used hypocotyl graft chimeras and found that a *HY5* scion permitted shoot-illumination promotion of root growth and NO_3^- uptake (versus a *hy5-526* scion; Figures 1E and 1F), suggesting that a HY5-dependent shoot-derived signal regulates root growth and NO_3^- uptake. To determine whether HY5 is (part of) this signal, we next expressed transgenes encoding HY5-GFP or myc-HY5 fusion proteins in *hy5* using non-tissue-specific *pHY5* [2], photosynthetic-tissue-specific *pCAB3* [16, 17], or phloem companion-cell-specific *pSUC2* promoters [18], finding that both HY5-GFP and myc-HY5 complemented the *hy5* phenotype (Figures S2C and S2D) and thus retain HY5 activity. We also found that *pHY5:HY5-GFP*, *pCAB3:HY5-GFP*, and *pSUC2:HY5-GFP* all restored shoot-illumination regulation of primary root growth to *hy5* (Figure 2A). Because *pCAB3*-driven expression is photosynthetic tissue specific, these observations suggest that *HY5* transcripts, HY5, or a HY5-dependent signal moves from shoot to root.

We next found that HY5-GFP was detectable throughout the roots of S(L)/R(D) *pHY5:HY5-GFP hy5* seedlings, but not in S(D)/R(D) (Figure 2B), suggesting that root HY5 abundance is regulated by shoot illumination and that HY5 is relatively stable in dark-grown roots. We additionally detected HY5-GFP in the roots of S(L)/R(D) *pCAB3:HY5-GFP hy5* seedlings, but not in S(D)/R(D) controls (Figure 2C). Because *HY5-GFP* transcripts are not detected in roots of *pCAB3:HY5-GFP hy5* seedlings (Figure S2D), this observation suggests that HY5 moves from shoot to root. Accordingly, whereas *myc-HY5* transcripts were detectable only in S(L)/R(D) shoots of *pCAB3:myc-HY5 hy5* plants (Figures 2D and S2D), myc-HY5 was detected in both shoots and roots of S(L)/R(D) plants (Figure 2E). This result was confirmed by detection of HY5-GFP in roots of S(L)/R(D)-grown *pCAB3:HY5-GFP hy5/hy5* graft chimeras (Figures 2F and S2E). Additional experiments with *pHY5:HY5-GFP hy5/hy5* graft chimeras detected HY5-GFP in S(L)/R(D)-grown roots (Figures S2F–S2H), further suggesting that HY5 moves from shoot to root.

We next expressed a fused HY5-GFP, TEV^{rs} (TEV protease recognition site), and double β-glucuronidase (2 × GUS) (2 × GUS-TEV^{rs}-HY5-GFP) protein from *pCAB3*. This protein was detected in shoots, but not in roots, of S(L)/R(D) plants, most likely because its relatively large size prevents shoot-root mobility (Figures 2G and S2I). However, co-expression of *35S:TEVP* (expressing the TEV protease) enabled cleavage at the TEV^{rs} [19], resulting in detection of HY5-GFP in shoots and roots (Figures 2G and S2I). These changes in HY5-GFP mobility were reflected in parallel effects on shoot-illumination-promoted primary root growth (Figure 2H) and NO_3^- uptake (Figure 2I). Furthermore, HY5-GFP is detected in roots of S(L)/R(D)-grown *pSUC2:HY5-GFP hy5* seedlings and *pSUC2:HY5-GFP hy5/hy5* graft chimeras (Figure S2J), indicating that HY5 is a shoot-root phloem-mobile signal that mediates light regulation of root growth and NO_3^- uptake.

Shoot-to-Root Translocated HY5 Activates *NRT2.1* Expression and NO_3^- Uptake

The HY5-GFP distribution conferred on *hy5* roots by *pHY5:HY5-GFP* (Figure 2B) differs from that due to *pCAB3:HY5-GFP* (Figure 2C) or *pSUC2:HY5-GFP* (Figure S2J) and that seen in roots of *pHY5:HY5-GFP hy5/hy5* (Figure S2F) or *pSUC2:HY5-GFP hy5/hy5* graft chimeras (Figure S2J). A *pHY5:HY5-GFP* root

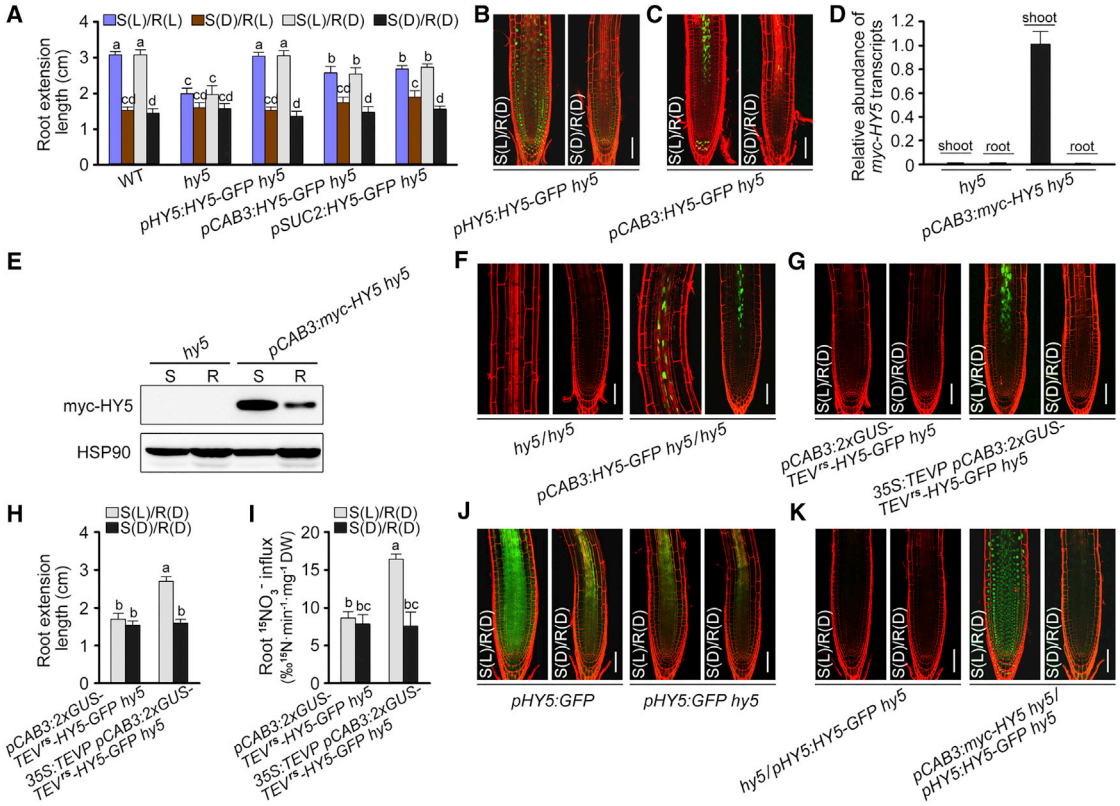

Figure 2. Shoot-to-Root Translocation of HY5 Regulates Root Growth and NO_3^- Uptake

(A) Differential shoot/root-illumination effects on primary root extension growth (seedling genotypes are as indicated) (see also Figures S2A–S2D).

(B) Distribution of HY5-GFP in *pHY5:HY5-GFP hy5* roots.

(C) Distribution of HY5-GFP in *pCAB3:HY5-GFP hy5* roots (see also Figure S2E).

(D) *myc-HY5* transcript abundance in the shoots and roots of 14-day-old plants (relative to that in *pCAB3:myc-HY5 hy5* shoots). Data are shown as mean ± SEM (n = 3).

(E) Immunological detection of myc-HY5 in shoots (S) and roots (R) of S(L)/R(D) plants, with HSP90 as a loading control (see Figures S2F–S2H for *pHY5:HY5-GFP hy5/hy5* graft chimeras).

(F) Distribution of HY5-GFP in the roots of shoot-illuminated *pCAB3:HY5-GFP hy5/hy5* graft chimeras.

(G) Detection of HY5-GFP in roots of shoot-illuminated *pCAB3:2 × GUS-TEV^{rs}-HY5-GFP hy5* plants expressing TEV protease (see also Figure S2I).

(H) Differential shoot/root-illumination effects on primary root extension growth of plants expressing TEV protease.

(I) Differential shoot/root-illumination effects on root $^{15}NO_3^-$ uptake of plants expressing TEV protease.

(J) Differential shoot/root-illumination effects on expression of a *pHY5:GFP* transgene in roots.

(K) Distribution of HY5-GFP in seedling roots (grafted as indicated) (see also Figure S2J).

(B, C, F, G, J, K) Scale bar, 50 μm.

(A, H, I) Data are shown as mean ± SEM (n = 30).

The same lowercase letter denotes a non-significant difference between means ($p < 0.05$). See also Figure S2 and Table S1.

genotype causes HY5-GFP to be detected throughout the root, whereas roots of *pCAB3:HY5-GFP hy5* and *pSUC2:HY5-GFP hy5* or *pHY5:HY5-GFP hy5/hy5* and *pSUC2:HY5-GFP hy5/hy5* chimeras exhibit a HY5-GFP location more closely associated with the root vasculature. This difference is most likely because HY5 activates root *HY5* expression [20]. First, shoot-illumination induction of root expression of a *pHY5:GFP* transgene (reporting *pHY5* activity by driving the expression of the *GFP* marker gene) is reduced in *hy5* (Figure 2J), suggesting that shoot-derived HY5 normally activates root *pHY5*. Second, HY5-GFP is detectable in roots of shoot-illuminated *pCAB3:myc-HY5 hy5/pHY5:HY5-GFP hy5* grafts, but not in roots of shoot-illuminated *hy5/pHY5:HY5-GFP hy5* grafts (Figure 2K). Third, electrophoretic mobility shift assays (EMSAs) and chromatin immunoprecipitation (ChIP) analysis using the roots of *pHY5:myc-HY5 hy5* seedlings confirmed binding of HY5 to *pHY5* [20] (Figures S3A and S3B). These observations indicate that shoot-root translocated HY5 activates root *HY5* via an auto-regulatory feedback loop and also explain the different patterns of HY5-GFP distribution conferred on *hy5* roots by *pHY5:HY5-GFP* (Figure 2B) versus *pCAB3:HY5-GFP* (Figure 2C) or *pSUC2:HY5-GFP* (Figure S2J).

We next found that shoot-illumination promotion of root *NRT2.1* transcript levels is largely abolished in *hy5* (Figure 3A). In addition, whereas shoot illumination partially promoted root *NRT2.1* transcript levels in *HY5/hy5* grafts, this effect was still further reduced in *hy5/HY5* grafts (Figure 3A). Further experiments showed that whereas either a *HY5* scion/*pHY5:HY5-GFP hy5* stock or a *pCAB3:HY5-GFP hy5* scion/*HY5* stock

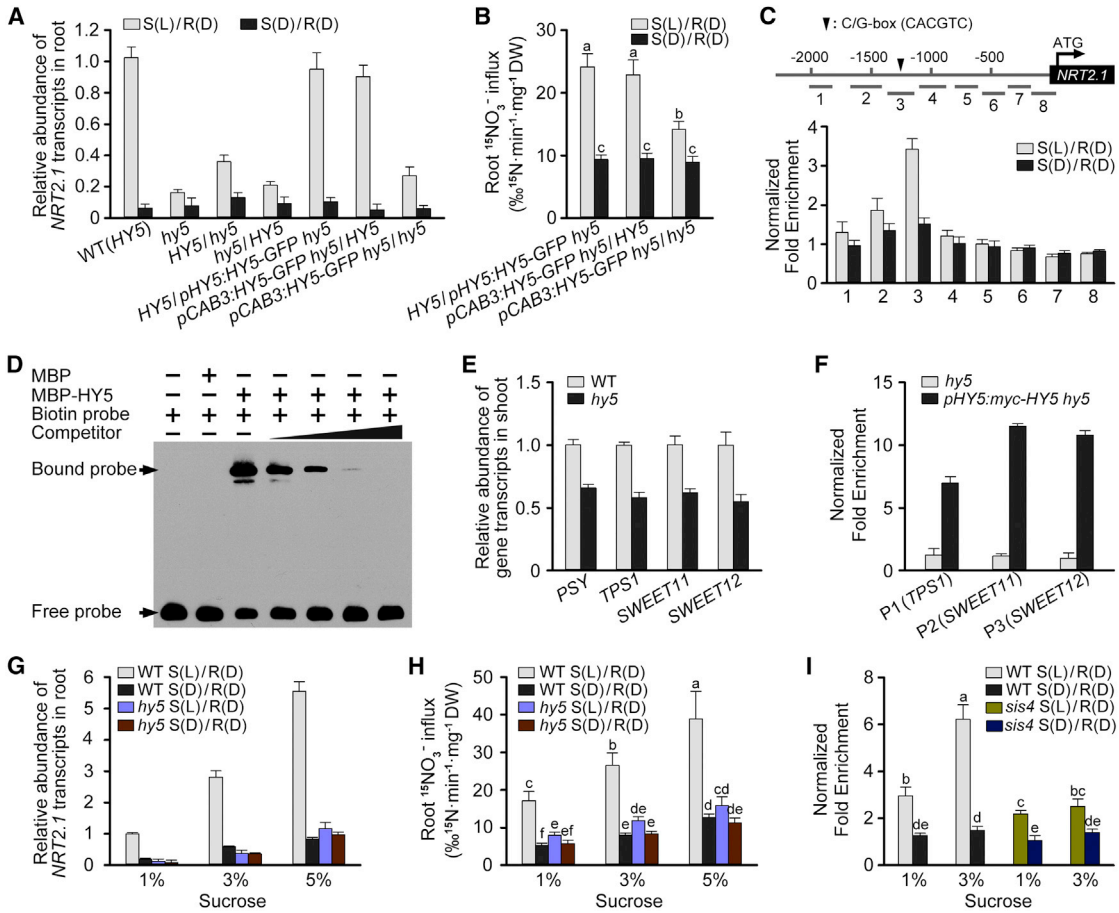

Figure 3. HY5 Coordinates N and C Metabolism

(A) *NRT2.1* transcript levels in primary seedling roots (genotypes/graft chimeras are as shown), with abundance relative to the level in WT roots. Data are shown as mean ± SEM (n = 3).

(B) Root NO_3^- uptake of graft chimeras. Data are shown as mean ± SEM (n = 30).

(C) *NRT2.1* promoter fragments used for ChIP analysis of extracts from 14-day-old *pHY5:myc-HY5 hy5* plants. Data are shown as mean ± SEM (n = 3). An arrow indicates C/G box sequence motif.

(D) Fragment 3 from (C) was incubated with MBP-HY5. Competition was performed with 10-, 20-, 50-, or 100-fold unlabeled probe excess.

(E) Relative abundance of *PSY*, *TPS1*, *SWEET11*, and *SWEET12* transcripts in 7-day-old seedlings. Values are expressed relative to WT level. Data are shown as mean ± SEM (n = 3).

(F) ChIP assays (see also Figures S3A and S3B). Fragments containing G box motifs in the *TPS1*, *SWEET11*, and *SWEET12* promoters were used for ChIP analysis of extracts from 14-day-old *pHY5:myc-HY5 hy5* (or control *hy5*) plants. Data are shown as mean ± SEM (n = 3).

(G) Sucrose affects shoot-illumination promotion of root *NRT2.1* transcript abundance [relative to abundance in WT S(L)/R(D) seedlings in 1% sucrose] (see also Figures S3C and S3H). Data are shown as mean ± SEM (n = 3).

(H) Sucrose affects shoot-illumination promotion of root $^{15}NO_3^-$ uptake (see also Figures S3D and S3I). Data are shown as mean ± SEM (n = 30).

(I) In vivo binding of HY5 to fragment 3 (see C) of the *NRT2.1* promoter. ChIP-PCR analysis was performed using 10-day-old *pHY5:myc-HY5 hy5* plants (see also Figures S3E–S3G). Data are shown as mean ± SEM (n = 3).

The same lowercase letter denotes a non-significant difference between means ($p < 0.05$). See also Figure S3 and Table S2.

permitted shoot-illumination-dependent elevation of root *NRT2.1* transcript levels to an extent similar to that seen in *HY5* plants, that of a *pCAB3:HY5-GFP hy5* scion/*hy5* stock was reduced versus that seen in *HY5* plants (Figure 3A). These differential effects were reflected in parallel effects on shoot illumination and NRT2.1-dependent NO_3^- uptake (Figure 3B) and relate to the need for a functional *HY5* in the root. ChIP and EMSA demonstrated both in vivo and in vitro binding of HY5 to the *NRT2.1* promoter (Figures 3C and 3D), indicating that HY5 directly regulates *NRT2.1* expression. Taken together, these results suggest that shoot-root mobile HY5 activates root *NRT2.1* via a mechanism that is amplified by auto-activation of root *HY5*, thereby increasing NO_3^- uptake.

Mobile HY5 Contributes to Maintain Homeostatic Balance of C and N Metabolism in Response to Ambient Light Conditions

Recent studies showed that HY5 modulates photosynthetic capacity in part via control of expression of chlorophyll biosynthesis and photosynthesis-related genes [21, 22]. For example,

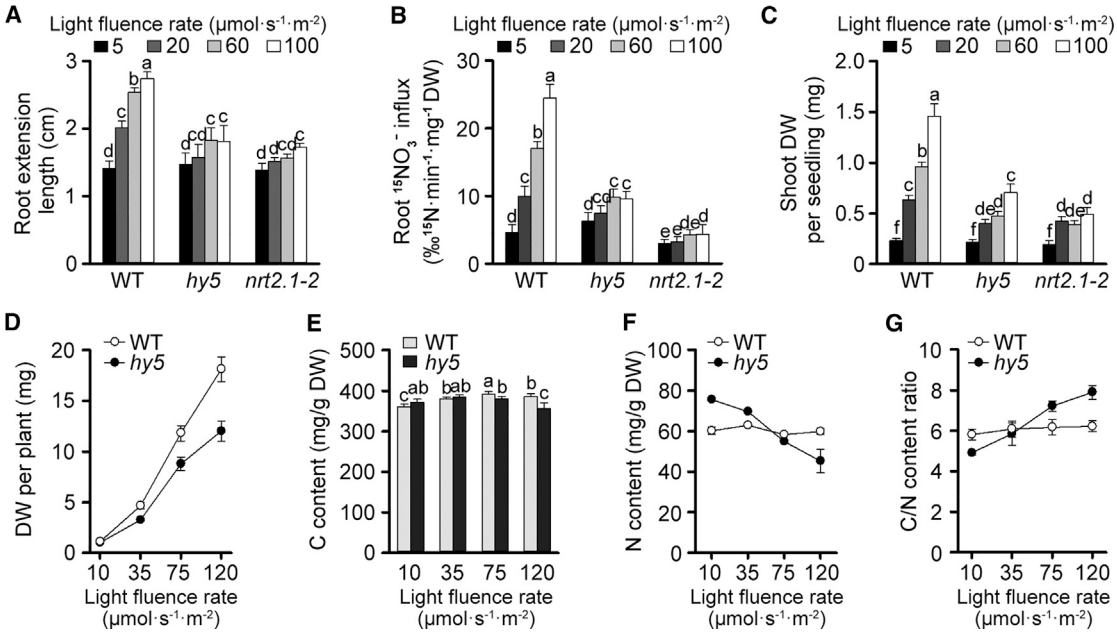

Figure 4. HY5 Coordinates Plant Growth and Nutrition in Responses to Fluctuating Light Environments

(A) Primary root extension lengths of seedlings grown in fluence rates as indicated. Data are shown as mean ± SEM (n = 30).

(B) $^{15}NO_3^-$ uptake of seedlings grown in fluence rates as indicated. Data are shown as mean ± SEM (n = 30).

(C) Seedling shoot biomass at different fluence rates. Data are shown as mean ± SEM (n = 30).

(D) Whole-plant biomass of plants grown in soil for 21 days (16 hr photoperiod) at different light fluence rates (see also Figure S4).

(E) C contents of plants shown in (D).

(F) N contents of plants shown in (D).

(G) C/N content ratio of 21-day-old plants grown in fluence rates as indicated.

(D–G) Data are shown as mean ± SEM (n = 16).

The same lowercase letter denotes a non-significant difference between means ($p < 0.05$). See also Figure S4.

HY5 promotes *PHYTOENE SYNTHASE* (*PSY*) expression by directly binding to the *PSY* promoter [22] (Figure 3E). Fixed C is predominantly transported to sink tissues (e.g., roots) through the phloem in the form of sucrose [23], and the trehalose precursor trehalose-6-phosphate (T6P) acts as a proxy for photosynthetic carbohydrate status [24]. We also found that HY5 affects both sucrose metabolism and shoot-root transport by promoting the expression levels of *TPS1*, a gene encoding trehalose-6-phosphate synthase [24], and *SWEET11* and *SWEET12* [23], genes encoding sucrose efflux transporters (Figure 3E). Further ChIP experiments confirmed in vivo binding of HY5 to the *TPS1*, *SWEET11*, and *SWEET12* promoters (Figure 3F). Thus, HY5 regulates both initial C fixation and subsequent movement of fixed C into phloem cells for shoot-root translocation.

Because C status regulates N status [7, 8], we next determined whether sugar level affects light-activated NRT2.1-dependent NO_3^- uptake. We found that both sucrose and glucose enhance the shoot-illumination promotion of root *NRT2.1* expression and NO_3^- uptake, effects that are largely abolished in *hy5* (Figures 3G, 3H, S3C, and S3D). Moreover, ChIP assays showed that sucrose promotes light-activated in vivo binding of myc-HY5 to the *NRT2.1* promoter and that this effect was abolished in the sugar-insensitive mutant *sis4* [25] (Figure 3I). Because neither *HY5-GFP* abundance nor HY5-GFP mobility is increased by sucrose (Figures S3E–S3G), increased HY5 levels are unlikely to contribute to sucrose-induced increases in the binding affinity of myc-HY5 to the *NRT2.1* promoter. Whatever the mechanism, sucrose induction of *NRT2.1* expression and NO_3^- uptake is dependent upon HY5 (Figures S3H and S3I). Taken together, these results indicate that HY5 responds to sugar signals in the regulation of NRT2.1-dependent NO_3^- uptake, thus contributing to the coordinated homeostatic balancing of C and N metabolism.

Because natural fluctuation in incident light fluence affects both C fixation and HY5 abundance [26, 27], we next determined the effect of increasing fluence (5–100 $\mu mol \cdot s^{-1} \cdot m^{-2}$) on seedling root growth and NO_3^- uptake. We found that increasing fluence promotes WT primary root extension growth (Figure 4A) and NO_3^- uptake (Figure 4B), that these effects are associated with a fluence-dependent increase in biomass accumulation (Figure 4C), and that they are largely abolished in *hy5* and *nrt2.1-2* mutant seedlings (Figures 4A and 4B and 4C). We next determined whether HY5 continues to coordinate light-responsive growth and C and N metabolism in more mature plants. First, as expected, increasing fluence increases the biomass of 21-day-old soil-grown WT plants (Figures 4D and S4), an effect that is reduced in *hy5* (Figure 4D). Next, we found that the whole-plant C content of 21-day-old WT and *hy5* plants remains relatively constant with increasing fluence (Figure 4E). In contrast, whereas WT whole-plant N content remains relatively constant, that of *hy5* falls markedly as fluence increases (Figure 4F). In consequence, lack of HY5 causes a fluence-dependent increase in the C/N content ratio, which remains relatively

constant in WTs (Figure 4G). These findings suggest that mobile HY5 regulates the coordination of shoot and root growth and C and N acquisition throughout the plant life cycle. In particular, HY5 maintains homeostatic balance of C and N metabolism at varying light fluence.

Conclusions

Although a previous study implicates phloem-mobile sucrose as a cotyledon-derived signal to control primary root elongation during early seedling development in *Arabidopsis* [28], the molecular mechanism of the shoot-root long-distance signaling regulating lateral root growth and N uptake remains unclear [29]. Here, we show that HY5 is a shoot-root mobile signal that mediates light-regulated coupling of shoot growth and C assimilation with root growth and N uptake. This coupling is achieved via HY5 regulation of C fixation in the shoot and via sucrose-enhanced promotion of HY5-dependent N uptake in the root. In consequence, HY5 mediates homeostatic regulation of whole-plant C versus whole-plant N status. HY5 is already known to integrate multiple phytohormonal (e.g., abscisic acid) and environmental (e.g., low temperature) signaling inputs in the control of plant growth and development [30, 31]. Our discovery that HY5 is a mobile signal adds further dimension to this knowledge. Our finding that HY5 mobility mediates homeostatic coordination of C and N metabolism enhances understanding of how plant C and N nutrient balance is maintained in fluctuating environments and suggests novel strategies for the improvement of nutrient-use efficiency in crops.

SUPPLEMENTAL INFORMATION

Supplemental Information includes Supplemental Experimental Procedures, four figures, and two tables and can be found with this article online at http://dx.doi.org/10.1016/j.cub.2015.12.066.

AUTHOR CONTRIBUTIONS

X.C. performed most of the experiments; Q.Y. and C.J. generated transgenic plants and analyzed the results; X.G. performed genetic screening; X.F designed the experiments; and X.F and N.P.H. wrote the manuscript. All authors have discussed the results and contributed to the manuscript.

ACKNOWLEDGMENTS

We thank H. Yang for the *hy5* allele in a Col-0 background, M. Schmid for the *p35S:TEVP* transgenic line, and X.W. Deng and K. Palme for their comments on the manuscript. This research was supported by grants from 973 Program from National Basic Research Program of China (2011CB915403 and 2013CB967302) and the National Natural Science Foundation (31130070 and 91117015).

Received: November 5, 2015
Revised: December 6, 2015
Accepted: December 23, 2015
Published: February 11, 2016

REFERENCES

1. Coruzzi, G., and Bush, D.R. (2001). Nitrogen and carbon nutrient and metabolite signaling in plants. Plant Physiol. *125*, 61–64.
2. Oyama, T., Shimura, Y., and Okada, K. (1997). The Arabidopsis HY5 gene encodes a bZIP protein that regulates stimulus-induced development of root and hypocotyl. Genes Dev. *11*, 2983–2995.
3. Osterlund, M.T., Hardtke, C.S., Wei, N., and Deng, X.W. (2000). Targeted destabilization of HY5 during light-regulated development of Arabidopsis. Nature *405*, 462–466.
4. Cerezo, M., Tillard, P., Filleur, S., Muños, S., Daniel-Vedele, F., and Gojon, A. (2001). Major alterations of the regulation of root NO_3^- uptake are associated with the mutation of *Nrt2.1* and *Nrt2.2* genes in Arabidopsis. Plant Physiol. *127*, 262–271.
5. Crawford, N.M. (1995). Nitrate: nutrient and signal for plant growth. Plant Cell *7*, 859–868.
6. Ho, C.H., Lin, S.H., Hu, H.C., and Tsay, Y.F. (2009). CHL1 functions as a nitrate sensor in plants. Cell *138*, 1184–1194.
7. Nunes-Nesi, A., Fernie, A.R., and Stitt, M. (2010). Metabolic and signaling aspects underpinning the regulation of plant carbon nitrogen interactions. Mol. Plant *3*, 973–996.
8. Matt, P., Geiger, M., Walch-Liu, P., Engels, C., Krapp, A., and Stitt, M. (2001). Elevated carbon dioxide increases nitrate uptake and nitrate reductase activity when tobacco is growing on nitrate, but increases ammonium uptake and inhibits nitrate reductase activity when tobacco is growing on ammonium nitrate. Plant Cell Environ. *24*, 1119–1137.
9. Lillo, C. (2008). Signalling cascades integrating light-enhanced nitrate metabolism. Biochem. J. *415*, 11–19.
10. Lian, H.L., He, S.B., Zhang, Y.C., Zhu, D.M., Zhang, J.Y., Jia, K.P., Sun, S.X., Li, L., and Yang, H.Q. (2011). Blue-light-dependent interaction of cryptochrome 1 with SPA1 defines a dynamic signaling mechanism. Genes Dev. *25*, 1023–1028.
11. Ang, L.H., Chattopadhyay, S., Wei, N., Oyama, T., Okada, K., Batschauer, A., and Deng, X.W. (1998). Molecular interaction between COP1 and HY5 defines a regulatory switch for light control of Arabidopsis development. Mol. Cell *1*, 213–222.
12. Little, D.Y., Rao, H., Oliva, S., Daniel-Vedele, F., Krapp, A., and Malamy, J.E. (2005). The putative high-affinity nitrate transporter NRT2.1 represses lateral root initiation in response to nutritional cues. Proc. Natl. Acad. Sci. USA *102*, 13693–13698.
13. Huang, N.C., Liu, K.H., Lo, H.J., and Tsay, Y.F. (1999). Cloning and functional characterization of an Arabidopsis nitrate transporter gene that encodes a constitutive component of low-affinity uptake. Plant Cell *11*, 1381–1392.
14. Masclaux-Daubresse, C., Daniel-Vedele, F., Dechorgnat, J., Chardon, F., Gaufichon, L., and Suzuki, A. (2010). Nitrogen uptake, assimilation and remobilization in plants: challenges for sustainable and productive agriculture. Ann. Bot. (Lond.) *105*, 1141–1157.
15. Liu, Q., Chen, X., Wu, K., and Fu, X. (2015). Nitrogen signaling and use efficiency in plants: what's new? Curr. Opin. Plant Biol. *27*, 192–198.
16. An, H., Roussot, C., Suárez-López, P., Corbesier, L., Vincent, C., Piñeiro, M., Hepworth, S., Mouradov, A., Justin, S., Turnbull, C., and Coupland, G. (2004). CONSTANS acts in the phloem to regulate a systemic signal that induces photoperiodic flowering of Arabidopsis. Development *131*, 3615–3626.
17. Corbesier, L., Vincent, C., Jang, S., Fornara, F., Fan, Q., Searle, I., Giakountis, A., Farrona, S., Gissot, L., Turnbull, C., and Coupland, G. (2007). FT protein movement contributes to long-distance signaling in floral induction of Arabidopsis. Science *316*, 1030–1033.
18. Imlau, A., Truernit, E., and Sauer, N. (1999). Cell-to-cell and long-distance trafficking of the green fluorescent protein in the phloem and symplastic unloading of the protein into sink tissues. Plant Cell *11*, 309–322.
19. Mathieu, J., Warthmann, N., Küttner, F., and Schmid, M. (2007). Export of FT protein from phloem companion cells is sufficient for floral induction in Arabidopsis. Curr. Biol. *17*, 1055–1060.
20. Abbas, N., Maurya, J.P., Senapati, D., Gangappa, S.N., and Chattopadhyay, S. (2014). Arabidopsis CAM7 and HY5 physically interact and directly bind to the HY5 promoter to regulate its expression and thereby promote photomorphogenesis. Plant Cell *26*, 1036–1052.

21. Kobayashi, K., Obayashi, T., and Masuda, T. (2012). Role of the G-box element in regulation of chlorophyll biosynthesis in Arabidopsis roots. Plant Signal. Behav. *7*, 922–926.

22. Toledo-Ortiz, G., Johansson, H., Lee, K.P., Bou-Torrent, J., Stewart, K., Steel, G., Rodríguez-Concepción, M., and Halliday, K.J. (2014). The HY5-PIF regulatory module coordinates light and temperature control of photosynthetic gene transcription. PLoS Genet. *10*, e1004416.

23. Chen, L.Q., Qu, X.Q., Hou, B.H., Sosso, D., Osorio, S., Fernie, A.R., and Frommer, W.B. (2012). Sucrose efflux mediated by SWEET proteins as a key step for phloem transport. Science *335*, 207–211.

24. Wahl, V., Ponnu, J., Schlereth, A., Arrivault, S., Langenecker, T., Franke, A., Feil, R., Lunn, J.E., Stitt, M., and Schmid, M. (2013). Regulation of flowering by trehalose-6-phosphate signaling in Arabidopsis thaliana. Science *339*, 704–707.

25. Laby, R.J., Kincaid, M.S., Kim, D., and Gibson, S.I. (2000). The Arabidopsis sugar-insensitive mutants *sis4* and *sis5* are defective in abscisic acid synthesis and response. Plant J. *23*, 587–596.

26. Moore, B., Zhou, L., Rolland, F., Hall, Q., Cheng, W.H., Liu, Y.X., Hwang, I., Jones, T., and Sheen, J. (2003). Role of the Arabidopsis glucose sensor HXK1 in nutrient, light, and hormonal signaling. Science *300*, 332–336.

27. Osterlund, M.T., Wei, N., and Deng, X.W. (2000). The roles of photoreceptor systems and the COP1-targeted destabilization of HY5 in light control of Arabidopsis seedling development. Plant Physiol. *124*, 1520–1524.

28. Kircher, S., and Schopfer, P. (2012). Photosynthetic sucrose acts as cotyledon-derived long-distance signal to control root growth during early seedling development in Arabidopsis. Proc. Natl. Acad. Sci. USA *109*, 11217–11221.

29. Forde, B.G., and Cole, J.A. (2003). Nitrate finds a place in the sun. Plant Physiol. *131*, 395–400.

30. Xu, D., Li, J., Gangappa, S.N., Hettiarachchi, C., Lin, F., Andersson, M.X., Jiang, Y., Deng, X.W., and Holm, M. (2014). Convergence of light and ABA signaling on the ABI5 promoter. PLoS Genet. *10*, e1004197.

31. Catalá, R., Medina, J., and Salinas, J. (2011). Integration of low temperature and light signaling during cold acclimation response in Arabidopsis. Proc. Natl. Acad. Sci. USA *108*, 16475–16480.

Current Biology, Volume *26*

Supplemental Information

Shoot-to-Root Mobile Transcription Factor HY5 Coordinates Plant Carbon and Nitrogen Acquisition

Xiangbin Chen, Qinfang Yao, Xiuhua Gao, Caifu Jiang, Nicholas P. Harberd, and Xiangdong Fu

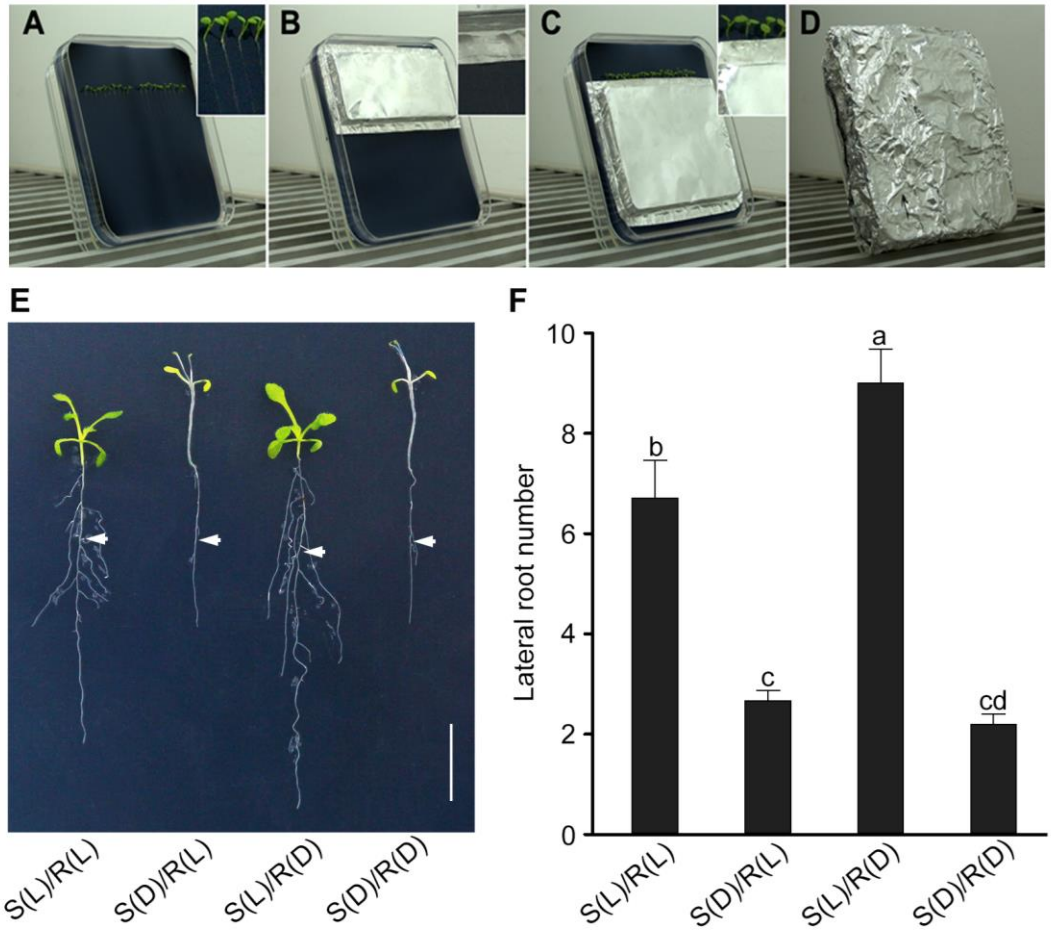

Figure S1. The effect of differential shoot/root illumination on lateral root development

3-day-old seedlings grown at 22 ℃ with a 16 h photoperiod were transferred to a new plate, then exposed to 3 days differential light treatment (100 μmol.s^{-1}.m^{-2}): (A) S(L)/R(L), shoot illuminated (S(L)) and root illuminated (R(L)). (B) S(D)/R(L), shoot dark-grown (S(D)) and root illuminated (R(L)). (C) S(L)/R(D), shoot illuminated (S(L)) and root dark-grown (R(D)). (D) S(D)/R(D), shoot dark-grown (S(D)) and root dark-grown (R(D)). (E) 3-day-old WT seedlings were transferred to a new plate, then exposed to 10d differential light treatment (100 μmol.s^{-1}.m^{-2}). Scale bar, 1 cm. (F) Lateral root production in different treatments. Data shown as mean ± s.e.m. (n = 30). The same lowercase letter denotes a non-significant difference between means (P < 0.05). Figure S1 is related to main Figure 1.

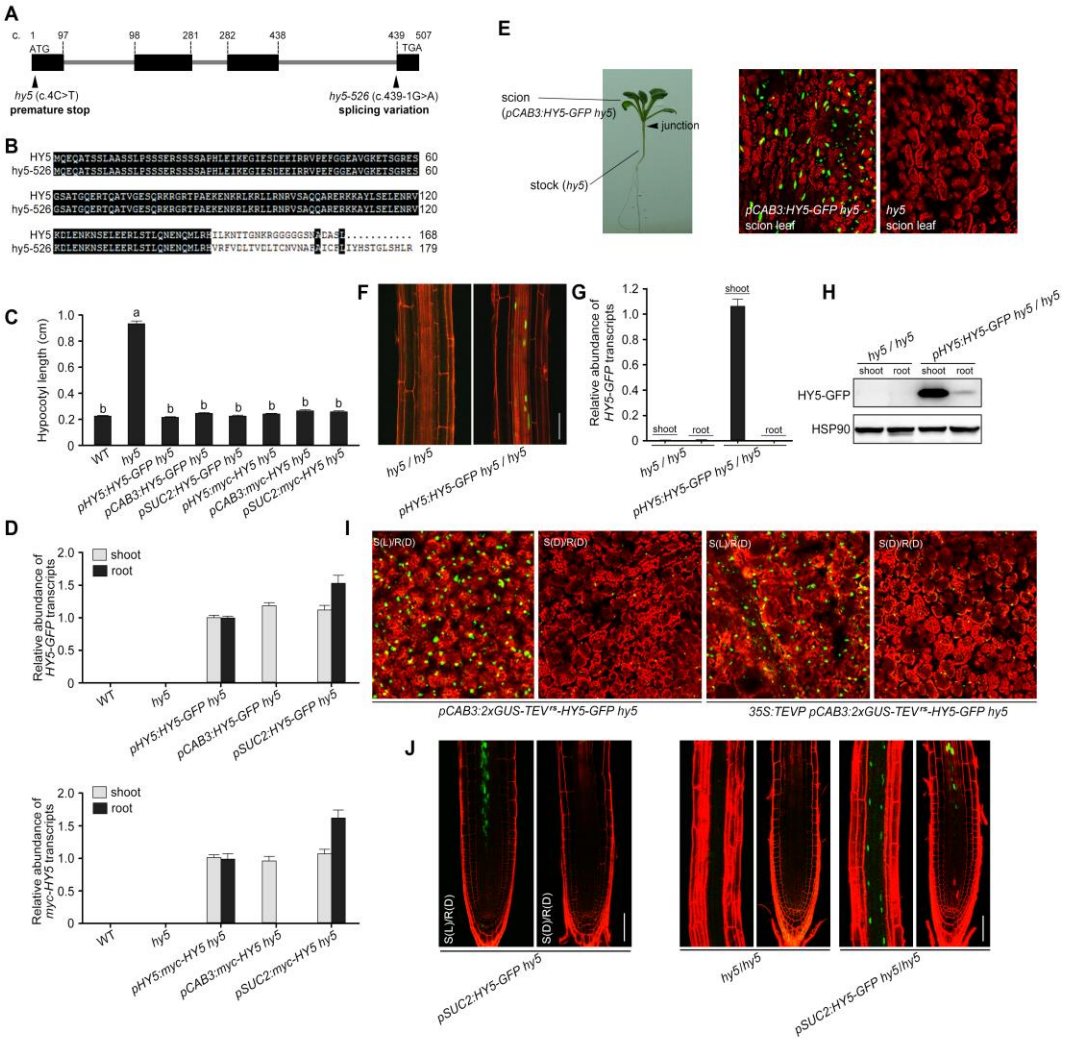

Figure S2. HY5 is a shoot-to-root translocated protein

(A) A representation of *HY5* coding sequence (c.) with bp 1 the A of the start ATG. *hy5-526* is a splice-site nucleotide substitution mutation (position as indicated). The allele referred to throughout this manuscript as *hy5* is a nucleotide substitution mutation creating a premature stop codon, and is thus a complete null allele. Dark grey boxes indicate exons, black lines indicate introns, and numbers indicate the exon sizes (bp). (B) Comparison of HY5 and mutant hy5-526 protein sequences. The numbers on the right indicate residue positions. Identical residues are indicated by dark grey boxes, and variant residues by light grey boxes. Aberrant splicing of *hy-526* results in a product lacking the HY5 C-terminal domain. (C) Hypocotyl lengths of light-grown 6-day-old seedlings (genotypes as indicated). Data shown as mean ± s.e.m. (n = 30). The same lowercase letter denotes a non-significant difference between means ($P < 0.05$). (D) Relative *HY5-GFP* and *myc-HY5* transcript abundance. Expression levels are expressed relative to abundance of Arabidopsis *actin2* mRNA. Data shown as mean ± s.e.m. (n =

3). (E) An example hypocotyl-graft chimera. HY5-GFP is detectable in the scion leaf of 10-day-old grafted plants (in a *pCAB3:HY5-GFP hy5* scion but not in a *hy5* scion). (F) HY5-GFP is detectable in roots of *pHY5:HY5-GFP hy5/hy5* graft chimeras 10 days following grafting. Scale bar, 50 μm. (G) *HY5-GFP* transcript abundance in shoots and roots of graft chimeras (relative to abundance in *pHY5:myc-HY5 hy5/hy5* shoots). Data shown as mean ± s.e.m. (n = 3). (H) Immunological detection of HY5-GFP in scion (shoot) and stock (root), with HSP90 loading control. (I) Distribution of GFP signal in leaves of shoot-illuminated *pCAB3:2×GUS-TEV^{rs}-HY5-GFP hy5* plants. (B) Distribution of GFP signal in leaves of shoot-illuminated *pCAB3:2×GUS-TEV^{rs}-HY5-GFP hy5* plants expressing the TEV protease. (J) HY5-GFP is detectable in roots of *pSUC2:HY5-GFP hy5* seedlings or *pSUC2:HY5-GFP hy5/hy5* seedling graft chimeras. Figure S2 is related to main Figure 2.

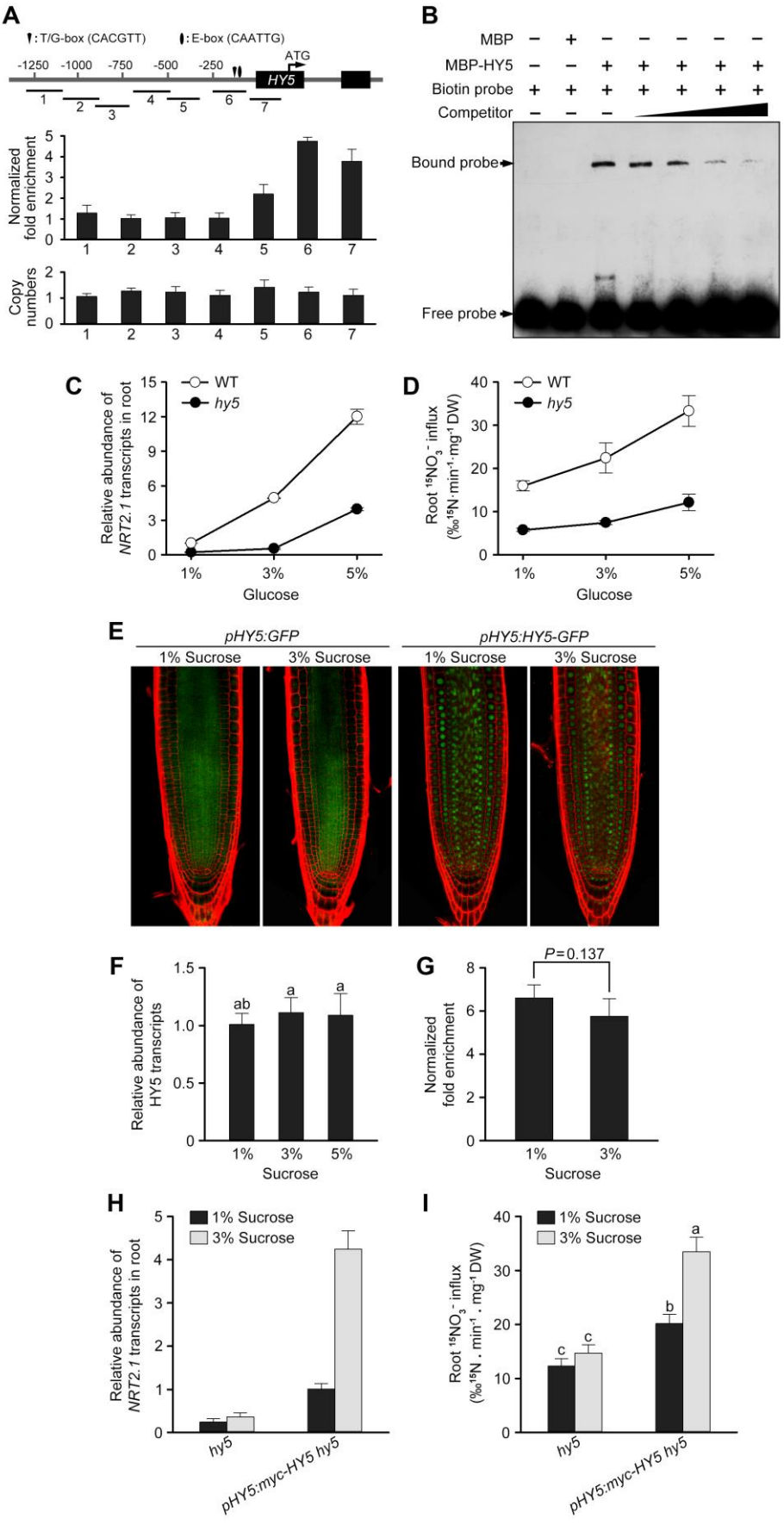
A
T/G-box (CACGTT)
E-box (CAATTG)
-1250 -1000 -750 -500 -250
ATG
HY5
1 2 3 4 5 6 7
Normalized fold enrichment
Copy numbers
B
MBP
MBP-HY5
Biotin probe
Competitor
Bound probe
Free probe
C
WT
hy5
Relative abundance of NRT2.1 transcripts in root
1% 3% 5%
Glucose
D
WT
hy5
Root 15NO3- influx (‰ 15N·min-1·mg-1 DW)
1% 3% 5%
Glucose
E
pHY5:GFP
pHY5:HY5-GFP
1% Sucrose
3% Sucrose
1% Sucrose
3% Sucrose
F
Relative abundance of HY5 transcripts
ab a a
1% 3% 5%
Sucrose
G
P=0.137
Normalized fold enrichment
1% 3%
Sucrose
H
1% Sucrose
3% Sucrose
Relative abundance of NRT2.1 transcripts in root
hy5
pHY5:myc-HY5 hy5
I
1% Sucrose
3% Sucrose
Root 15NO3- influx (‰ 15N . min-1 . mg-1 DW)
c c b a
hy5
pHY5:myc-HY5 hy5

Figure S3. A mobile HY5 auto-activates root *HY5*, and also regulates *NRT2.1* expression and NO_3^- uptake in response to levels of carbohydrate photosynthate

(A) ChIP assays. The diagram depicts the putative *HY5* promoter and fragments (1-7) used for ChIP analysis. ChIP-PCR was performed using 14-day-old *pHY5:myc-HY5 hy5* plants. Data shown as mean ± s.e.m. (n = 3). (B) EMSA assays. A T/G-box-motif-containing *HY5* promoter fragment (fragment 6 from A), was incubated with MBP-HY5 as indicated. Competition for HY5 binding was performed with 10×, 20×, 50× and 100× unlabeled probes containing the T/G-box motif, respectively. (C) *NRT2.1* transcript abundance in S(L)/R(D) roots of WT and *hy5* seedlings. Transcript levels are expressed relative to abundance of *Arabidopsis actin2*. Data shown as mean ± s.e.m. (n = 3). (D) $^{15}NO_3^-$ uptake of 7-day-old WT and *hy5* seedling roots. Data shown as mean ± s.e.m. (n = 10). (E) The effect of sucrose level on *HY5* transcription (as visualized by GFP expression driven by a *pHY5:GFP* transgene) and HY5 stability (HY5-GFP expressed from *pHY5:HY5-GFP*) in roots. Scale bar, 50 μm. (F) The effect of sucrose level on root *HY5* transcript abundance. Transcript levels are expressed relative to the abundance of *Arabidopsis actin2* mRNA. Data shown as mean ± s.e.m. (n = 3). (G) ChIP-PCR analysis performed using 10-day-old *pHY5:myc-HY5 hy5* plants grown on 1/2MS medium containing 1% or 3% sucrose. Enrichment of DNA fragment 6 of the *HY5* promoter shown in fig. S8 was determined by qRT-PCR analysis. Data shown as mean ± s.e.m. (n = 3). A Student's *t*-test was used to generate the *P* values. (H) Levels of *NRT2.1* transcripts in sucrose-treated *hy5* and *pHY5:myc-HY5 hy5* roots. Transcript levels are expressed relative to abundance of *Arabidopsis actin2*. Data shown as mean ± s.e.m. (n = 3). (I) Rates of $^{15}NO_3^-$ uptake in sucrose-treated *hy5* and *pHY5:myc-HY5 hy5* roots. Data shown as mean ± s.e.m. (n = 30). The presence of the same lowercase letter denotes a non-significant difference between means ($P < 0.05$). Figure S3 is related to main Figure 3.

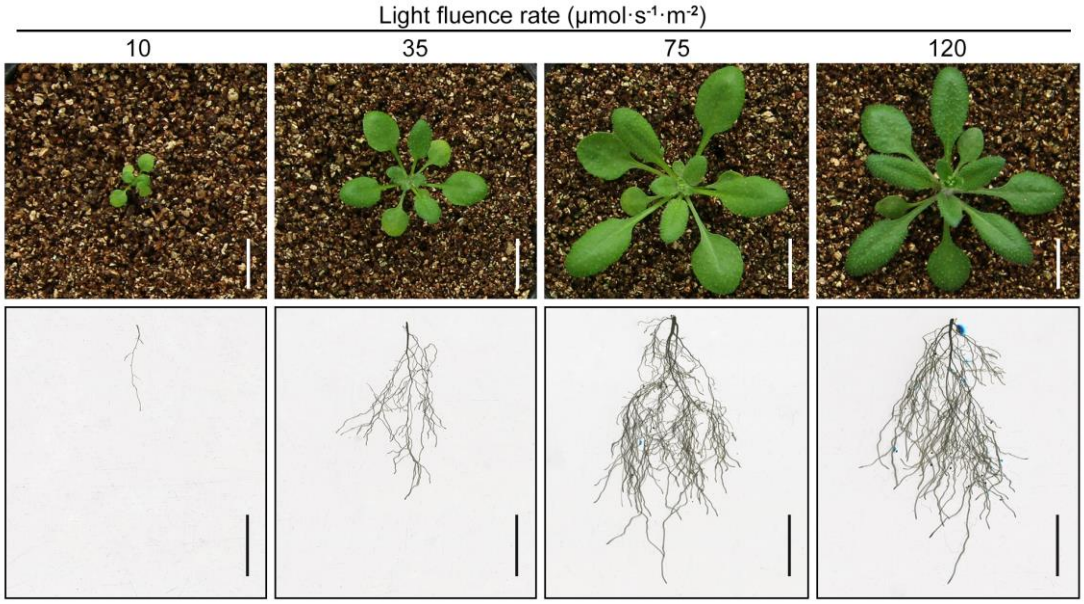

Figure S4. The effects of increasing light fluence rates on plant growth

The shoot (top panel) and root (lower panel) systems of WT plants grown in soil for 21 days (16 h photoperiod) at different light fluence rates are shown. Scale bar, 1 cm. Figure S4 is related to main Figure 4.

Supplemental tables

Table S1. Primer sequences used for DNA constructs and qRT-PCR analysis.

Primer Name	Primer sequence (5′ to 3′)
HY5-GFP-F	GATCTAGAATGCAGGAACAAGCGACTAG
HY5-GFP-R	CAGTCGACAAGGCTTGCATCAGCATTAG
GFP-F	AAGTCGACATGGTGAGCAAGGGCGAGGAG
GFP-R	CACTGCAGTTACTTGTACAGCTCGTCCAT
pHY5-F	GTCCATGGCTTCGTCGTCAGGATTAT
pHY5-R	CGGGTACCTTTTCTTACTCTTTGAAGATC
pSUC2-F	CGCCATGGTTTGTCATACATTTATTTGCCACAAG
pSUC2-R	GCGGTACCTTTGACAAACCAAGAAAGTAAGAAAAAAA
pCAB3-F	GACCATGGAATCAAGAGAAAATGTGATTCTCGG
pCAB3-R	CGCGGTACCGAAACTTTTTGTGTTTTTTTTTTTTTTTG
myc-HY5-F	GAGGATCCATGCAGGAACAAGCGACTAG
myc-HY5-R	GGTCTAGATCAAAGGCTTGCATCAGCAT
GUS-F1	GAGGTACCATGGATCTGACTAGTTT
GUS-R1	TTAGATCTGCTAGCTTGTTTGCCT
GUS-F2	GAAGATCTGATCTGACTAGTTTACGTC
GUS-TEV^{rs}-R2	ATGGTACCGCCGCTTCCAGAACCTGAACCCTGGAAGTACAAGTT CTCTCCAGAACCTGATCCAGAGCTAGCTTGTTTGCCTCCCTGCTG
TEV^{rs}-R2	ATGGTACCGCCGCTTCC
TEVP-F	ATGTTGTTTAAGGGACCACGTGAT TA
TEVP-R	TCAGTCACGATGAATTCCCGGCGAGT
qActin2-F	CTGGATCGGTGGTTCCATTC
qActin2-R	CCTGGACCTGCCTCATCATAC
qHY5-F	GAACGAGAACCAGATGCTTAGAC
qHY5-R	TGCAATATTAGCTCTCACATCCC
OCS-R	CATAGGCGTCTCGCATATCTC
qHY5-GFP-F	CAGAACGAGAACCAGATGCTTAG
qHY5-GFP-R	CAGATGAACTTCAGGGTCAGC
qNRT1.1-F	TCTAAGACCGCTTCAACGGATCG
qNRT1.1-R	ACTGTTGGACCATGAGCGTGTG
qNRT2.1-F	AACAAGGGCTAACGTGGATG
qNRT2.1-R	CTGCTTCTCCTGCTCATTCC
qPSY-F	GACACCCGAAAGGCGAAAGG
qPSY-R	CAGCGAGAGCAGCATCAAGC
qTPS1-F	GGTCATTTCTTGGGGAAGGA
qTPS1-R	TCTCCTGATGATGACTTGGC
qSWEET11-F	GCGAACAAGTGTACCTGCGG
qSWEET11-R	GGGTACACGTGGTGGTTGGT
qSWEET12-F	TCGTCCGATCGGTGAACACA
qSWEET12-R	ACTAGTACACGTGGACAATGGTGA

Table S1 is related to main Figure 2

Table S2. Primer sequences used for ChIP-PCR and EMSA assays.

Primer Name	Primer sequence (5′ to 3′)
HY5 fragment 1-F	GGCAGCTTAAAAGACTGGCTT
HY5 fragment 1-R	ATCACAACAAAACCATCCGTTATC
HY5 fragment 2-F	TTAAAAATCTGGCAGCTGAGGTT
HY5 fragment 2-R	CTTTTACTTTTTCCTTAGGTTCGAC
HY5 fragment 3-F	AGATGTTGTGGTCGAACCTAAGG
HY5 fragment 3-R	GTGAGATAGAGCATTCAAGTAACATAG
HY5 fragment 4-F	GTTTGATGATGCTGTGAATAGAATG
HY5 fragment 4-R	TGACGACAATGTTGATGAGTTTCT
HY5 fragment 5-F	CAGAAACTCATCAACATTGTCGTC
HY5 fragment 5-R	CCGCCATAAACCAAACAAAGT
HY5 fragment 6-F	TTCACGACACTTTTGAAAGCACTGCC
HY5 fragment 6-R	CAAGGATCCAAAGGCAATTGAG
HY5 fragment 7-F	ATTCACTCTCGATATCCGTTCG
HY5 fragment 7-R	AGAGAGAGAGGGAAAGATTTGTTG
NRT2.1 fragment 1-F	TTTACAAAGTGGTTCCTTCACGA
NRT2.1 fragment 1-R	CCAACAAATTAAGGATCTTCGG
NRT2.1 fragment 2-F	CTGGATGACATTAAAGTTCATACTTC
NRT2.1 fragment 2-R	GTACCGGACAAAAGAGAATCCT
NRT2.1 fragment 3-F	GAGAAAAGATAATGAGCTCATCGAA
NRT2.1 fragment 3-R	GTGCGGTGGATTGATATGTAGA
NRT2.1 fragment 4-F	AAATTCAGATCCGCTAGCTACTAC
NRT2.1 fragment 4-R	CGTATGTCAATGTATATGTGATGG
NRT2.1 fragment 5-F	CGATTTCAATTTTTCACACCGA
NRT2.1 fragment 5-R	AGTATTCACAAAAGGGGAAGATG
NRT2.1 fragment 6-F	ACAGTTACAATGACAAAGATAACCC
NRT2.1 fragment 6-R	CTTAAGGTTTAAAAGTTTGGTCCTC
NRT2.1 fragment 7-F	TTAGCCTATCCTGTATCACTGTATG
NRT2.1 fragment 7-R	AGGTTGCCGATATCCTTCCA
NRT2.1 fragment 8-F	TTGGTGATAAGCGAGAGACTAGG
NRT2.1 fragment 8-R	TCTTTGCAAGTTTGAGATTTGATTC
P1-TPS1 fragment-F	ACCCCTTACTTGTTAGTGGTTGAA
P1-TPS1 fragment-R	GGTATGGACAGAGATGTTGTTGGT
P2-SWEET11 fragment-F	AGAGCTAAAGTGAAAACGGCATAAT
P2-SWEET11 fragment-R	TGACGACATTCTGGAATTTGCT
P3-SWEET12 fragment-F	TTGCATTGTGTTTAATTACGGC
P3-SWEET12 fragment-R	GGTCACTGATACTTATGACGGATAG
HY5 probe	GCTAACCAGATCTAACGGCTAAAATCCACCCACGTTCCAA TCTCAATTGCCTTTGGATCCTTGTAT
NRT2.1 probe	TTATCAAATCCCAACTTGTTGGAAATTTGACACGTCAGCG AGATTGATCGATACGCACTTAGTCGT

Table S2 is related to main Figure3

Supplemental Experimental Procedures

Plant materials and growing conditions

Arabidopsis seeds were imbibed at 4 ℃ for three days, then plated on 1/2MS medium. Emerging seedlings were exposed to a 16 h photoperiod at 22 ℃. Experiments involving seedling grafting were performed as previously described [S1].

Plasmid constructs

HY5 cDNA was amplified and subcloned into the *pCaMV35S:nos* vector [S2]. The sequences of the *HY5, SUC2* and *CAB3* promoters were amplified and subcloned into the *pCaMV35S:nos* vector, as were both the *HY5* promoter and the *GFP* coding sequence to generate the *pHY5:GFP* expression cassette. The *HY5* coding sequence was cloned into the *pSK-N-Tagged-myc* vector [S3], and then subcloned into the *pCaMV35S:nos* vector. To make the *pCAB3:2×GUS-TEV^{rs}-HY5-GFP* fusion construct, the TEV recognition site (TEV^{rs}) was fused to the 3′-end of the 2×GUS coding sequence via PCR, and the PCR product was introduced into *pCAB3:HY5-GFP* vector. The TEV protease was amplified and cloned into *pCaMV35S:nos* vector [S2]. To construct the *pHY5:HY5-GFP* transgene, the *HY5* coding sequence was cloned into the *pHY5:GFP* construct. Primer sequences used for PCR amplifications are given in Table S1.

Transcript analysis

Total RNA was extracted using the TRIzol reagent (Invitrogen, New York, USA), and reverse transcribed using an M-MLV Reverse Transcriptase kit (Promega, Wisconsin, USA). qRT-PCR analysis was performed as described previously [S4]. Each experiment was represented by three biological replicates with at least three technical replicates per biological replicate. *Arabidopsis actin2* was used as a reference gene. The relevant primers are given in Table S1.

Immunoblot analysis

Preparations of crude protein were obtained by extracting in 50 mM Tris-HCl (pH 7.5), 150 mM KCl, 10 mM $MgCl_2$, 1 mM EDTA, 10% glycerol, 0.1% NP-40, 1×complete protease inhibitor (Roche). An aliquot was electrophoresed through a 10% (w/v) SDS–polyacrylamide gel and transferred on to a Hybond ECL nitrocellulose membrane. Subsequent handling of the membrane followed an established protocol [S5]. The myc-

HY5 and HY5-GFP fusion proteins were detected using anti-myc (Santa Cruz Biotechnology, Santa Cruz, USA) and anti-GFP (Roche Diagnostics GmbH, Germany) antibodies respectively, and signals were visualized using the SuperSignal West Pico Chemiluminescent Substrate (Thermo Fisher Scientific, Waltham, USA).

Measurement of total carbon and nitrogen content

Dehydrated plant tissue was milled, and a high temperature combustion process [S6] used to determine the total carbon and nitrogen content of the powdered material using an Elementar Vario PYRO Cube analyzer (Elementar Analysensysteme GmbH, Frankfurt, Germany).

$^{15}NO_3$-uptake activity assay

Root $^{15}NO_3^-$ influx was assayed as described elsewhere [S7]. Roots were dried overnight at 80 ℃, and the ^{15}N content was measured using the ANCA-MS system (PDZ Europa Ltd).

ChIP-PCR assays

hy5 and *pHY5:myc-HY5 hy5* seedlings were grown on 1/2MS plates for 14 days. A 2 g aliquot of plant tissue was then fixed by formaldehyde cross-linking. The ChIP assay used anti-myc antibodies (Santa Cruz Biotechnology, Santa Cruz, USA) as previously described [S8]. Enrichment of DNA fragments was determined by qRT-PCR analysis. Three independent biological replicates were performed. The relevant primer sequences are given in Table S2.

EMSA assays

HY5 cDNA was amplified and cloned into the pMAL™-c2X vector (New England Biolabs, Ipswich, USA). MBP and MBP-HY5 fusion proteins were purified according to the manufacturer's instructions. The DNA probes were amplified and labeled with biotin at their 3-end, using a biotin label kit (Invitrogen, New York, USA). DNA gel-shift assays were performed using the LightShift Chemiluminescent EMSA Kit (Thermo Fisher Scientific, Waltham, USA). The primer sequences used are given in Table S2.

Supplemental references

S1. Corbesier, L., Vincent, C., Jang, S., Fornara, F., Fan, Q., Searle, I., Giakountis, A., Farrona, S., Gissot, L., Turnbull, C., and Coupland, G. FT protein movement contributes to long-distance signaling in floral induction of Arabidopsis. Science *316*, 1030-1033.

S2. Wang, S., Wu, K., Yuan, Q., Liu, X., Liu, Z., Lin, X., Zeng, R., Zhu, H., Dong, G., Qian, Q., Zhang, G., and Fu, X. (2012). Control of grain size, shape and quality by OsSPL16 in rice. Nat. Genet. *44*, 950-954.

S3. Wang, S., Li, S., Liu, Q., Wu, K., Zhang, J., Wang, S., Wang, Y., Chen, X., Zhang, Y., Gao, C., Wang, F., Huang, H., and Fu, X. (2015). The *OsSPL16-GW7* regulatory module determines grain shape via the control of cell division patterning and simultaneously improves rice yield and grain quality. Nat. Genet. *47*, 949-954.

S4. Sun, H., Qian, Q., Wu, K., Luo, J., Wang, S., Zhang, C., Ma, Y., Liu, Q., Huang, X., Yuan, Q., Han, R., Zhao, M., Dong, G., Guo, L., Zhu, X., Gou, Z., Wang, W., Wu, Y., Lin, H., and Fu, X. (2014). Heterotrimeric G proteins regulate nitrogen-use efficiency in rice. Nat. Genet. *46*, 652-656.

S5. Jiang, C., Gao, X., Liao, L., Harberd, N.P., and Fu, X. (2007). Phosphate starvation root architecture and anthocyanin accumulation responses are modulated by the gibberellin-DELLA signaling pathway in Arabidopsis. Plant Physiol. *145*, 1460-1470.

S6. Matejovic, I. (1993). Determination of carbon, hydrogen, and nitrogen in soils by automated elemental analysis (dry combustion method). Commun. Soil Sci. Plant Anal. *24*, 2213-2222.

S7. Ho, C.H., Lin, S.H., Hu, H.C., and Tsay, Y.F. (2009). CHL1 functions as a nitrate sensor in plants. Cell *138*, 1184-1194.

S8. Gendrel, A.V., Lippman, Z., Martienssen, R., and Colot, V. (2005). Profiling histone modification patterns in plants using genomic tiling microarrays. Nat. Methods. *2*, 213-218.